A Theoretical Investigation of Dimethyl Carbonate Synthesis on Cu−Y Zeolite

Xiaobo Zheng and Alexis T. Bell*

Department of Chemical Engineering, University of California, Berkeley, California 94720

Received: December 3, 2007; In Final Form: January 8, 2008

A theoretical analysis of the mechanism of dimethyl carbonate (DMC) synthesis via oxidative carbonylation of methanol on Cu-exchanged Y zeolite, Cu−Y, was explored using density functional theory. These calculations show that methanol adsorbs in the presence of oxygen to form coadsorbed methoxide and hydroxide species and dimethoxide species on extraframework Cu^+ cations. DMC can form by CO addition to the former species to produce monomethyl carbonate species, which then react with additional methanol or by CO addition to dimethoxide species to form DMC directly. The turnover frequency for DMC synthesis is estimated to be 1.2×10^{-5} s^{-1} for the reaction conditions used in the experimental work of Zhang and Bell (*J. Catal.*, in press). This value compares very closely with that observed, 5×10^{-5} s^{-1}. The calculated value of the apparent activation energy is 15.0 kcal/mol, in good agreement with that measured experimentally, 14.8 kcal/mol. The effects of methanol and oxygen on the adsorption of CO have also been examined. CO adsorbs on Cu^+ cations with a heat of adsorption of 18.7 kcal/mol; the vibrational frequency of the adsorbed CO is 2134 cm^{-1}. Coadsorption of CO and molecular methanol reduces the heat of CO adsorption to 10.1 kcal/mol and shifts the C−O frequency to 2117 cm^{-1}. However, formation of Cu^+-bound methoxide, when CH_3OH and O_2 are present together with CO, completely inhibits the adsorption of CO. These findings are in very good agreement with experimental observation.

Introduction

Dimethyl carbonate (DMC) can be used potentially as a fuel additive to replace methyl *tert*-butyl ether (MTBE), a precursor for synthesis of carbonic acid derivatives, as a methylating agent to replace methyl halides and dimethyl sulfate, and as an intermediate in the synthesis of polycarbonates and isocyanates.[1−3] Cu-exchanged zeolite are known to be active catalysts for oxidative carbonylation of methanol to dimethyl carbonate[4−8] via the reaction $2CH_3OH + CO + {}^1/_2O_2 \rightarrow (CH_3O)_2CO + H_2O$. The highest activity and selectivity to DMC has been reported for Cu−Y and Cu−X, whereas Cu−ZSM-5 and Cu−MORD show much lower activities and selectivities to DMC. The high activity of Cu−Y has been found to be associated with the lower heat of adsorption for CO on Cu cations in this zeolite than for Cu cations exchanged into ZSM-5 or MORD.[6−8] Studies of the kinetics of DMC synthesis have shown that the rate of formation of this product is roughly first order in CO and nearly zero order in methanol and oxygen.[6−8] Consistent with these findings, mechanistic investigations suggest that the rate-limiting step is the addition of CO to form either carbomethoxide or monomethyl carbonate (MMC) species.[4−9] A recent transient-response infrared spectroscopy study provides strong evidence that MMC is the precursor and that the subsequent reaction of MMC with methanol to form DMC is rapid.[9] This work has also shown that while CO adsorbs strongly on Cu cations exchanged into Y zeolite in the absence of methanol and oxygen, when methanol and oxygen were both present, the formation of methoxide species occurs very rapidly, leading to the displacement of adsorbed CO.

The aim of the present investigation was to analyze the energetics of DMC synthesis on Cu−Y. The results of this effort were used to understand the thermodynamics of methoxide species formation from methanol and oxygen in the presence of CO, the mechanism of MMC formation via the reaction of CO with adsorbed methoxide species, and the mechanism by which DMC is formed as a final product. The turnover frequency for DMC synthesis was estimated on the basis of the reported calculations, as was the apparent activation energy.

Computational Methods

Electronic energies of reactants, products, and transition states were determined using density functional theory (DFT). The B3LYP functional was used to describe electron exchange and correlation, and the 6-31G* basis set was used to locate optimized ground-state and transition-state structures. All geometry optimizations were done using the Gaussian 03 software.[10] After a particular molecular structure was optimized to a stationary point (transition state or minimum energy structure), its energy was further refined by a single-point calculation using the 6-311+G** basis set. Cu was described using the cc-PVTZ basis set of Balabanov et al.[11] The quantum chemical methods used in this work were validated by comparing the calculated and observed dissociation energies of $Cu(CO)_x$ in our previous study.[12]

The "growing string method" developed by Peters et al.[13] was used to locate the transition state connecting two minimum energy structures. In this method a minimum energy path connecting the reactant and product is estimated without making an initial guess for the reaction path. The point with highest energy on this reaction path was taken to be an estimate of the transition-state geometry. This structure was further converged to that of the exact saddle point by the transition-state-finding algorithm implemented in the Gaussian 03 software.[10] Because of the large number of degrees of freedom in the system (over 100), determination of the transition-state estimates was difficult

* To whom correspondence should be addressed: E-mail: bell@cchem.berkeley.edu.

10.1021/jp711415g CCC: $40.75
Published on Web 03/12/2008

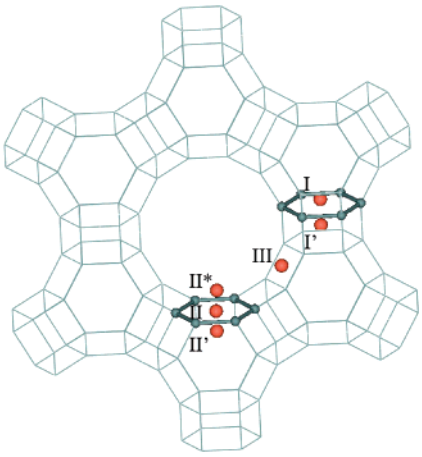

Figure 1. Possible Cu sites of Y zeolite.

even with the GSM. To overcome this difficulty, an iterative partial optimization approach (IPOA) was used.[14] All transition states reported here were verified to have only one imaginary frequency.

Choice of Active Site. The three-dimensional structure of zeolite Y is formed by connecting sodalite units with hexagonal prisms. The larger void space enclosed by six sodalite cages and six hexagonal prisms known as supercage has a diameter of around 12 Å. The unit cell of Y zeolite is cubic and contains 192 T (Si or Al) atoms. As seen in Figure 1, Cu cations can occupy various cation-exchange sites in Y zeolite.[15] Site I is located at the center of a hexagonal prism, whereas site I′ is located in a sodalite cage adjacent to a hexagonal face shared by an hexagonal prism and a sodalite cage. Site II is located in a supercage adjacent to a hexagonal face of sodalite cage shared by a sodalite cage and a supercage, whereas site II′ is located in sodalite cage adjacent to a hexagonal face shared by a sodalite cage and a supercage. Site II* is similar to site II but displaced toward the supercage. Site III is located in a supercage adjacent to a four-membered ring of a sodalite cage. Because it is very difficult for CO to diffuse inside the hexagonal prism, only sites II and III are accessible to CO adsorption. Experimental work by Drake and co-workers[16] has shown that the exchange of H−Y with CuCl vapor at elevated temperature results in the quantitative exchange of all protons by Cu^+ cations, so that Cu/Al = 1.0. On the basis of an analysis of temperature-programmed reduction data, these authors concluded that 3.4 Cu/unit cell occupy site III while 17.2 Cu/unit cell occupy site II*. Since most of the Cu^+ cations are located at site II* cation-exchange positions, Cu^+ cations located at this position were used to represent the catalytically active site.

Cu^+ cations at site II* were represented by the six T atom cluster shown in Figure 2. Si atoms were fixed in their crystallographic positions and all dangling bonds were saturated with hydroxyl groups and terminal H atoms were oriented in the direction of next tetrahedral atom. The Si to Al ratio was set to be 2 to reflect that used in the experimental studies, Si/Al = 2.5, by replacing two of the Si atoms with Al cations. Since the extra Al brings a negative charge to the cluster, a proton was added to compensate this charge. In its minimum-energy configuration, the Cu^+ cation is coordinated to three O atoms of the zeolite framework, with Cu−O bond distances of 1.87, 1.91, and 2.43 Å, This coordination is in good agreement with that determined from an analysis of extended X-ray absorption fine structure (EXAFS) data reported by Zhang et al.[8]

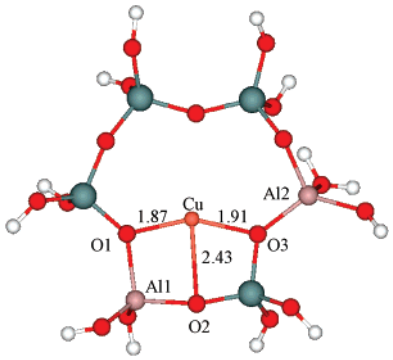

Figure 2. Cluster model for Cu^+ associated with site II* in Cu−Y.

Results

Energetics of DMC Synthesis. The proposed reaction mechanism for DMC formation is illustrated in Figure 3. The sequence of individual reaction steps illustrated shown is suggested by the experimental work of Zhang and Bell.[9] The Cu^+ site (see Figure 2a) is denoted with an asterisk. The notation (X)* and (X)(Y)* is used to represent a Cu^+ cation interacting with species X or X and Y.

The first reaction step in this mechanism is the molecular adsorption of methanol

$$* + CH_3OH \rightarrow (CH_3OH)* \qquad (1)$$

Reaction 1 is exothermic and endoergic, $\Delta E^0 = -11.2$ kcal/mol and $\Delta G^0 = 3.0$ kcal/mol. The presence of this species is clearly observed experimentally by the appearance of infrared absorption bands at 2952, 2844, and 1458 cm^{-1}.[9] When O_2 is present in the feed, with or without CO, the molecularly adsorbed CH_3OH is converted rapidly to methoxide species $(CH_3O)(OH)*$, which are evidenced by the appearance of infrared bands at 2925, 2824, and 1458 cm^{-1}. Under steady-state reaction conditions, methoxide species and molecularly adsorbed methanol are the dominant species observed by in situ infrared spectroscopy.[9] Thus, it is reasonable to assume that the reaction 2, shown below, rapidly reaches equilibrium

$$(CH_3OH)* + {}^1/_2O_2 \rightarrow (CH_3O)(OH)* \qquad (2)$$

The value of ΔE for this reaction is −47.2 kcal/mol, making the reaction strongly exothermic. The Gibbs free energy change is $\Delta G^0 = -5.4$ kcal/mol, so that the reaction is exoergic.

$(CH_3O)(OH)*$, produced in reaction 2 can react further with CH_3OH to form the dimethoxide species, $(CH_3O)_2*$

$$(CH_3O)(OH)* + CH_3OH \rightarrow (CH_3O)_2* + H_2O \qquad (3)$$

for which $\Delta E^0 = -2.4$ kcal/mol and $\Delta G^0 = -1.1$ kcal/mol. $(CH_3O)_2*$ cannot be discerned experimentally because the vibrational spectra of the CH_3O group in this species and in $(CH_3O)(OH)*$ are virtually the same.

DMC can be formed via two processes. The first involves the reaction of CO with $(CH_3O)(OH)*$ via reaction 4 to produce MMC

$$(CH_3O)(OH)* + CO \rightarrow (CH_3OCOOH)* \qquad (4)$$

This reaction is strongly exothermic with $\Delta E^0 = -71.9$ kcal/mol, and ΔG^0 is calculated to be −57.0 kcal/mol. The calculated transition-state structure of this step is illustrated in Figure 4. The location of this type of transition state structure is extremely difficult to find owing to the very large degrees of freedom in

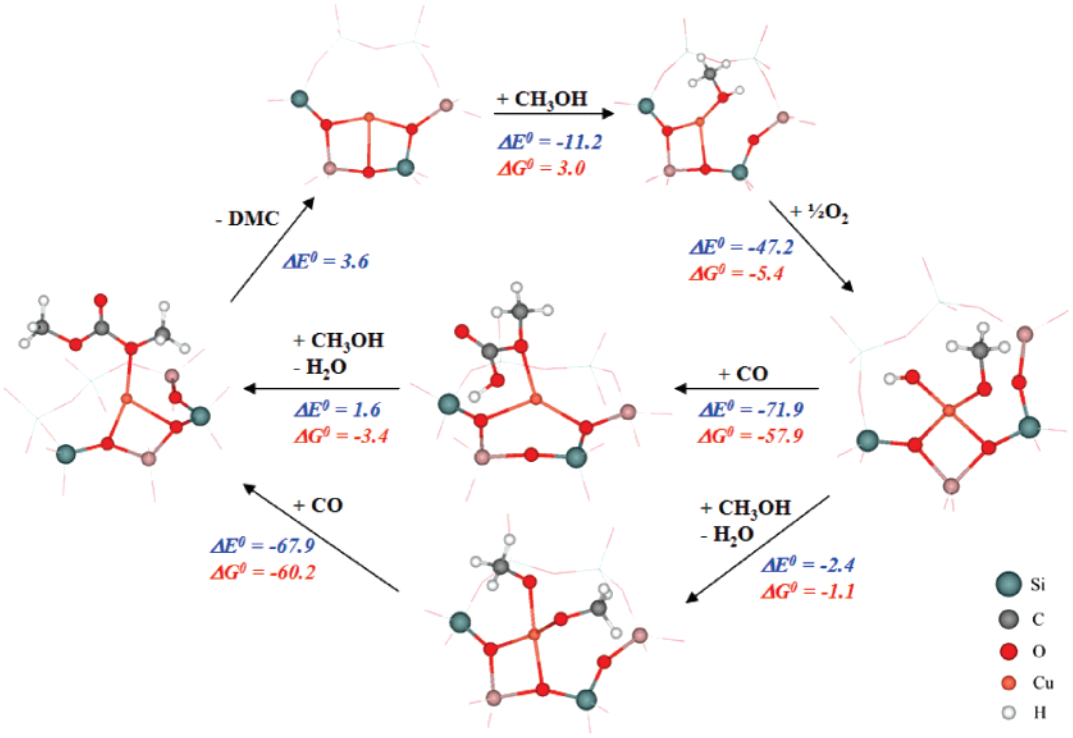

Figure 3. Proposed reaction mechanism for DMC synthesis.

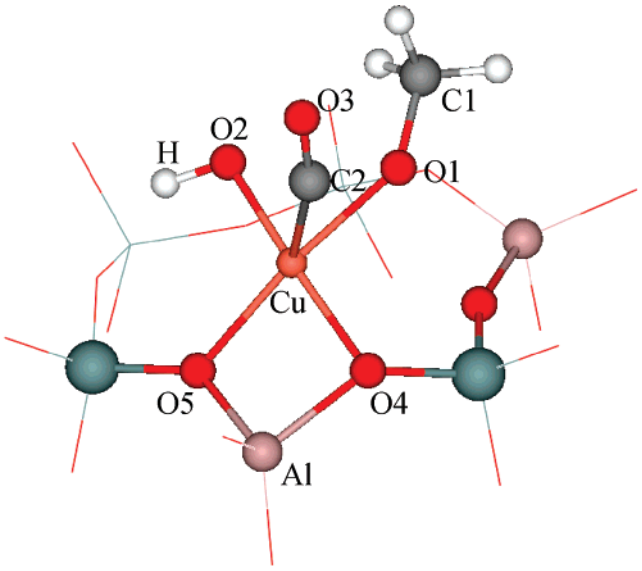

Figure 4. Structure of TS1.

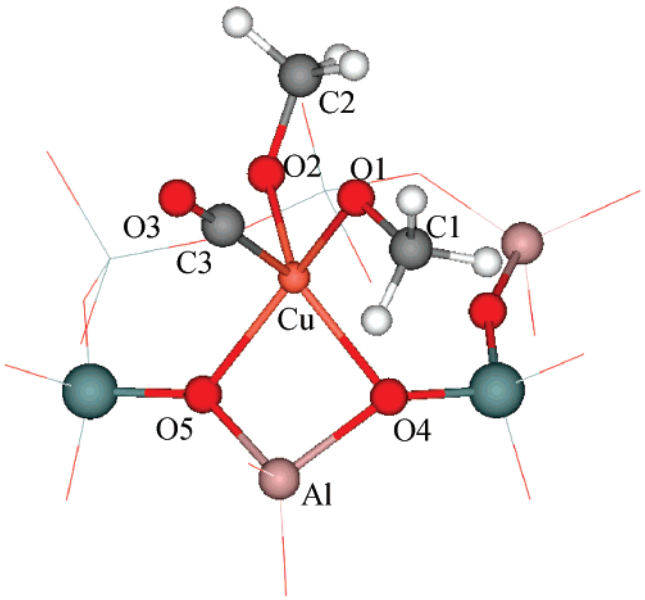

Figure 5. Structure of TS2.

the system. CO inserts into the Cu−OCH_3 bond with a C2−Cu distance of 2.14 Å and a C2−O1 distance of 1.80 Å. The O1−Cu distance is greatly increased from 1.77 to 2.85 Å to accommodate the insertion of CO. $(CH_3OCOOH)^*$ can react further with methanol to form adsorbed DMC and H_2O via reaction 5. The activation energy and free energy are calculated to be $\Delta E_a^0 = 13.2$ kcal/mol and $\Delta G_a^0 = 23.6$ kcal/mol.

Once formed, MMC react rapidly with CH_3OH to form adsorbed DMC

$$(CH_3OCOOH)^* + CH_3OH \rightarrow (CH_3OCOOCH_3)^* + H_2O \quad (5)$$

This reaction step is almost thermal neutral with $\Delta E^0 = 1.6$ kcal/mol.

The second pathway by which DMC can be formed involves the addition of CO to $(CH_3O)_2^*$ to produces adsorbed DMC, $(CH_3OCOOCH_3)^*$, via reaction 6. The calculated structure of $(CH_3OCOOCH_3)^*$ is similar to isomer (b) reported by Zecchina co-workers[17] for DMC adsorbed in Na−Y

$$(CH_3O)_2^* + CO \rightarrow (CH_3OCOOCH_3)^* \quad (6)$$

This reaction step is significantly exothermic with $\Delta E^0 = -67.9$ kcal/mol. The transition state structure of this later CO insertion step is shown in Figure 5. The C3−Cu bond distance in the transition state structure is 2.19 Å, and the C3−O1 bond distance is 1.81 Å. The O1−Cu bond distance increases from 1.76 to 2.04 Å. The activation energy and the Gibbs free energy of activation are $\Delta E_a^0 = 15.0$ kcal/mol and $\Delta G_a^0 = 24.9$ kcal/mol, respectively. DMC is released into the gas phase via reaction 7, for which $\Delta E^0 = 3.6$ kcal/mol

$$(CH_3OCOOCH_3)^* \rightarrow CH_3OCOOCH_3 + * \qquad (7)$$

The energetics determined for reactions 1−7 are qualitatively consistent with the transient-response infrared and mass spectrometry observations reported recently by Zhang and Bell.[9] The authors reported that at 403 K methanol and oxygen react rapidly on the Cu^+ cations in Cu−Y to form methoxide groups. Upon removal of methanol and oxygen from the gas phase and introduction of CO, the adsorbed methoxide groups slowly react to form adsorbed MMC, detected by infrared spectroscopy, and gas-phase DMC, detected by mass spectrometry. The appearance of these species provides good support for the progress of reactions 4 and 6 plus 7. If the gas phase is next purge of CO and methanol and oxygen are reintroduced, adsorbed MMC reacts rapidly to form DMC, observations which point to reactions 5 and 7. It was also observed that exposure of the Cu−Y to gas-phase DMC at 403 K lead to the appearance of infrared bands for adsorbed MMC and methoxide species, products that would form via the reverse of reactions 7 and 5.

The experimental work of Bell and co-workers[8,9] suggests that, under steady-state reactions conditions, the Cu^+ sites of Cu−Y are saturated with monomethoxide and, possibly, dimethoxide species, $(CH_3O)(OH)^*$ and $(CH_3O)_2^*$, and that the rate-limiting step is the addition of DMC to these species. To test this hypothesis, the Gibbs free energies for reactions 1−3 were used to calculate the equilibrium occupancy of Cu^+ cations as $(CH_3OH)^*$, $(CH_3O)(OH)^*$, and $(CH_3O)_2^*$. For these calculations it was assumed that the temperature is 403 K and that the partial pressures of methanol and water vapor are 0.12 and 0.012 atm, respectively, since these are representative of values used in the experimental studies.[8,9] The resulting values are $\theta_{(CH_3OH)^*} = 0$, $\theta_{(CH_3O)(OH)^*} = 0.03$, and $\theta_{(CH_3O)_2^*} = 0.97$. The TOF for DMC formation can then be represented by the equation

$$\mathrm{TOF} = k_4\theta_{(CH_3O)(OH)^*}P_{CO} + k_6\theta_{(CH_3O)_2^*}P_{CO} \qquad (8)$$

where P_{CO} is the partial pressure of CO. The values of the rate coefficients k_4 and k_6, appearing in eq 8, can be determined from transition-state theory from the following relationship[18−20]

$$k = \frac{k_b T}{h}\frac{Q_{TS}}{Q_R}\exp(-\Delta E_a/RT) \qquad (9)$$

where k_b is Boltzman's constant, h is Planck's constant, T is temperature, and Q_{TS} and Q_R are the partition functions for the transition state and the reactant state, respectively. The values of k_4 and k_6 determined from eq 9 are 1.0×10^{-3} s^{-1} atm^{-1} and 3.2×10^{-5} s^{-1} atm^{-1}, respectively, at 403 K. Introducing these values of k_4 and k_6 into eq 8 and taking $P_{CO} = 0.2$ atm, the value used in the experimental work[9] yields a value of TOF $= 1.2 \times 10^{-5}$ s^{-1}. The predicted value of TOF is 4 times less than that measured experimentally, 5×10^{-5} s^{-1}.[9] The apparent activation energy can also be determined from eq 8. The value obtained this way is 15.0 kcal/mol, which is only slightly higher than the experimental value of 14.8 kcal/mol[9] but well within the accuracy of both the calculated and measured values.

Zhang and Bell[8,9] have reported that in the absence of methanol and oxygen, CO adsorbs on Cu^+ cation in Cu−Y and exhibits a well-defined band at 2139 cm^{-1}. When methanol is present together with CO, the CO band is red-shifted to 2117 cm^{-1} and is reduced in intensity. The authors suggested that this change was due to the co-adsorption of molecular CH_3OH and CO, and that charge transfer from the oxygen atom of adsorbed CH_3OH to the Cu^+ cation resulted in weakening of the heat of CO adsorption and the red shift in the frequency of the C−O vibrations. The latter effect was attributed to an increase in charge transfer in the π^* antibonding orbital of CO. When O_2 was introduced together with CO and CH_3OH, methoxide species formed, and the intensity of the band for adsorbed CO decreased substantially relative to that observed for CO adsorption in the absence of CH_3OH and O_2, and the position of the C−O vibration shifted further to 2117 cm^{-1}. Zhang and Bell proposed that the observations made when CO was adsorbed in the presence of CH_3OH and O_2 could be attributed to the formation of methoxide species, which were more strongly bound to Cu^+ cations than CO. The present study was extended in an effort to explain the effects of methanol and oxygen on the adsorption of CO.

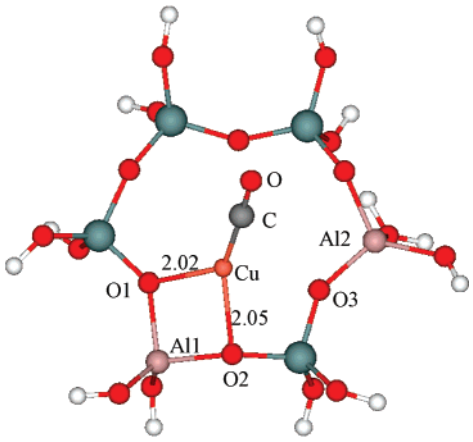

Figure 6. Structure of adsorbed CO.

Figure 6 illustrates the structure of adsorbed CO. Comparison with Figure 2 shows that, upon CO adsorption, the Cu^+ migrates from its original position and the Cu−O coordination number decreases from three to two with Cu−O bond distances of 2.02 and 2.05 Å. The reduction in Cu−O coordination number from three to two upon CO adsorption is fully consistent with the X-ray absorption near-edge structure and EXAFS observations reported previously by Zhang et al.[8] The geometry of CO adsorbed at site II and the change in Cu−O coordination number from three to two upon CO adsorption have also been reported Rejmak et al. in a recent theoretical study.[21] The calculated CO binding energy is 18.7 kcal/mol, and the C−O vibrational frequency is 2132 cm^{-1}. Both the calculated binding energy and C−O vibrational frequency are in good agreement with those reported experimentally, 16−19 kcal/mol and 2139−2145 cm^{-1} [8,22,23] and those calculated theoretically using a hybrid quantum mechanics/ interatomic potential method, 16 kcal/mol and 2141 cm^{-1}.[21] When methanol is coadsorbed as a molecule, the binding energy for CO reduces to 10.1 kcal/mol and the C−O vibrational frequency shifts to 2117 cm^{-1}. While the binding energy of CO coadsorbed with methanol has not been measured, the C−O vibrational frequency is in very good agreement with that seen experimentally, 2120 cm^{-1}.[8,9] When O_2 is introduced along with CH_3OH and $(CH_3O)(OH)^*$ species are formed but CO will not bind to with complex, since the value of ΔE^0 is large and positive.

Conclusions

The synthesis of DMC via oxidative carbonylation of methanol over Cu−Y initiates by reaction of molecularly adsorbed CH_3OH with O_2 to form mono- and dimethoxide species, $(CH_3O)(OH)^*$ and $(CH_3O)_2^*$. DMC is then formed via two reaction pathways. The first involves CO reaction with $(CH_3O)(OH)^*$ to form MMC, $(CH_3COOH)^*$, which then react

with CH_3OH to produce DMC. The second process involves the reaction of CO with $(CH_3O)_2$* to produce DMC directly. Experimental studies have shown that the formation of methoxide species reaches equilibrium rapidly but that the addition of CO is rate limiting. By use of these assumptions and the thermodynamic and rate parameters obtained in the present study, the rate of DMC formation and the associated activation energy are estimated to be 1.2×10^{-5} s^{-1} and the activation energy is estimated to be 15.0 kcal/mol, for the reaction conditions reported by Zhang and Bell.[8] These values agree well with the observed values for the rate and activation energy, 5×10^{-5} s^{-1} and 14.8 kcal/ mol.

The influence of CH_3OH and O_2 on the adsorption of CO on Cu^+ cation in Cu−Y was investigated. CO adsorbs on Cu^+ cation located in site II* cation-exchange sites with a calculated adsorption energy of −18.4 kcal/mol and a calculated C−O vibrational frequency of 2134 cm^{-1}, in very close agreement with experimental observation. Coadsorption of CO and molecular methanol reduces the CO adsorption energy to −10.1 kcal/mol and red-shifts the C−O band to 2117 cm^{-1}; however, when O_2 is also present in the gas phase, the formation of methoxide groups bound to Cu^+ cations completely inhibits the adsorption of CO. These predictions are also in excellent agreement with experimental observation.

Acknowledgment. This work was supported by the Methane Conversion Cooperative funded by BP. Computations were carried out on a Dell cluster of the Molecular Graphics and Computation Facility at the University of California, Berkeley. Supercomputer time on the NCSA HP/Convex Exemplar SPP-2000 at the University of Illinois at Urbana−Champaign was provided by the National Computational Science Alliance.

References and Notes

(1) Ono, Y. *Appl. Catal. A* **1997**, *155*, 133.
(2) Pacheco, M. A.; Marshall, C. L. *Energy Fuels* **1997**, *11*, 2.
(3) Ono, Y. *Pure Appl. Chem.* **1996**, *68*, 367.
(4) King, S. T. *J. Catal.* **1996**, *161*, 530.
(5) King, S. T. *Catal. Today* **1997**, *33*, 173.
(6) Anderson, S. A.; Root, T. W. *J. Catal.* **2003**, *217*, 396.
(7) Anderson, S. A.; Root, T. W. *J. Mol. Catal. A* **2004**, *220*, 247.
(8) Zhang, Y. H.; Drake, I. J.; Briggs, D. N.; Bell, A. T. *J. Catal.* **2006**, *244*, 219.
(9) Zhang, Y.; Bell, A. T. *J. Catal.* **2008**, in press.
(10) Frisch, M. J.; Trucks, G. W.; Schlegel, H. B.; Gill, P. M. W.; Johnson, B. G.; Robb, M. A.; Cheeseman, J. R.; Keith, T.; Petersson, G. A.; Montegomery, J. A.; Raghavachari, K.; Al-Laham, M. A.; Zakrzewski, V. G.; Ortiz, J. V.; Foresman, J. B.; Cioslowski, J.; Stefanov, B. B.; Nanayakkara, A.; Challacombe, M.; Peng, C. Y.; Ayala, P. Y.; Chen, W.; Wong, M. W.; Andres, J. L.; Replogle, E. S.; Gomperts, R.; Martin, R. L.; Fox, D. J.; Binkley, J. S.; Defrees, D. J.; Baker, J.; Stewart, J. P.; Head-Gordon, M.; Gonzalez, C.; Pople, J. A. *Gaussian 03*, revision B.04; Gaussian, Inc.: Pittsburgh, PA, 2003.
(11) Balabanov, N. B.; Peterson, K. A. *J. Chem. Phys.* **2005**, *123*, 064107.
(12) Zheng, X.; Zhang, Y.; Bell, A. T. *J. Phys. Chem. C* **2007**, *111*, 13442.
(13) Peters, B.; Heyden, A.; Bell, A. T.; Chakraborty, A. *J. Chem. Phys.* **2004**, *120*, 7877.
(14) Zheng, X.; Bell, A. T. *J. Phys. Chem. C*, in press.
(15) Smith, J. V. *Adv. Chem. Phys.* **1971**, 171.
(16) Drake, I. J.; Zhang, Y. H.; Briggs, D.; Lim, B.; Chau, T.; Bell, A. T. *J. Phys. Chem. B* **2006**, *110*, 11654.
(17) Bonino, F.; Damin, A.; Bordiga, S.; Selva, M.; Tundo, P.; Zecchina, A. *Angew. Chem., Int. Ed.* **2005**, *44*, 4774.
(18) Levine, I. N. *Quantum Chemistry*, 5th ed.; Prentice Hall: Upper Saddle River, New Jersey, 2000.
(19) Leach, A. R. *Molecular Modeling*; Longman: Essex, England, 1998.
(20) Holbrook, K. A.; Pilling, M. J.; Robertson, S. H. *Unimolecular Reactions*, 2nd ed; John Wiley & Sons: New York, 1996.
(21) Rejmak, P.; Sierka, M.; Sauer, J. *Phys. Chem. Chem. Phys.* **2007**, *9*, 5446.
(22) Datka, J.; Kozyra, P. *J. Mol. Struct.* **2005**, *744*, 991.
(23) Palomino, G. T.; Bordiga, S.; Zecchina, A.; Marra, G. L.; Lamberti, C. *J. Phys. Chem. B* **2000**, *104*, 8641.